JPE 19-2-7

https://doi.org/10.6113/JPE.2019.19.2.403
ISSN(Print): 1598-2092 / ISSN(Online): 2093-4718

EMI Noise Source Reduction of Single-Ended Isolated Converters Using Secondary Resonance Technique

Zhangyong Chen†, Yong Chen*, Qiang Chen*, Wei Jiang*, and Rongqiang Zhong*

†,*Institute for Electric Vehicle Driving System and Safety Technology, School of Automation Engineering, University of Electronic Science and Technology of China, Chengdu, China

Abstract

Aiming at the problems of large dv/dt and di/dt in traditional single-ended converters and high electromagnetic interference (EMI) noise levels, a single-ended isolated converter using the secondary resonance technique is proposed in this paper. In the proposed converter, the voltage stress of the main power switch can be reduced and the voltage across the output diode is clamped to the output voltage when compared to the conventional flyback converter. In addition, the peak current stress through the main power switch can be decreased and zero current switching (ZCS) of the output diode can be achieved through the resonance technique. Moreover, the EMI noise coupling path and an equivalent model of the proposed converter topology are presented through the operational principle of the proposed converter. Analysis results indicate that the common mode (CM) EMI noise and the differential mode (DM) EMI noise of such a converter are deduced since the frequency spectra of the equivalent controlled voltage sources and controlled current source are decreased when compared with the traditional flyback converter. Furthermore, appropriate parameter selection of the resonant circuit network can increase the equivalent impedance in the EMI coupling path in the low frequency range, which further reduces the common mode interference. Finally, a simulation model and a 60W experimental prototype of the proposed converter are built and tested. Experimental results verify the theoretical analysis.

Key words: Electromagnetic interference (EMI), Secondary-side resonance, Single-ended converter, Soft switching

I. INTRODUCTION

Recently, power switching converters [1]-[5] have received a lot of attention in many regions, such as switch mode power supplies, LED drivers, renewable energy conversion systems, electric vehicles and so on. The flyback or forward converter has been widely used in low power applications, due to its simple structure, low cost and easy control. However, due to the fast transitions of power switching devices, the electromagnetic interference (EMI) problem in these isolated converters is very serious and may lead to an inability to satisfy electromagnetic interference standards. Thus, a lot of research has been carried out to relieve or eliminate these problems.

There are common-mode (CM) and differential-mode (DM) conducted EMI in power switching converters. The character of the noise source and coupling path for a flyback converter is given in Fig. 1, and common-mode noise prediction can be achieved in [6]. The analysis results in [6] indicate that common mode noise is composed of a factor of three coupling paths, i.e. the coupling capacitance of the transformer, parasitic capacitor of the main power switch and parasitic capacitor of the output diode. A lot of studies have attempted to solve the EMI problem of isolated converters [7]-[24]. According to previous analyses, there are three groups of methods to reduce the CM EMI noise for single-ended isolated converters. Firstly, EMI filter or active filtering methods [7]-[9] have been used in the input-side of DC/DC converters and the common mode conducted noise can be attenuated through bypassing the propagation path. In addition, using a hybrid filter, the size and weight of an EMI filter can be reduced in [9]. Secondly, CM

Manuscript received Jun. 3, 2018; accepted Jan. 16, 2019
Recommended for publication by Associate Editor Jongwon Shin.
†Corresponding Author: zhang_yong_ch@126.com
Tel: +86-28-66360106, Univ. Electronic Sci. & Tech. China (UESTC)
*Institute for Electric Vehicle Driving System and Safety Technology, School of Automation Engineering, Univ. Electronic Sci. & Tech. China (UESTC), China

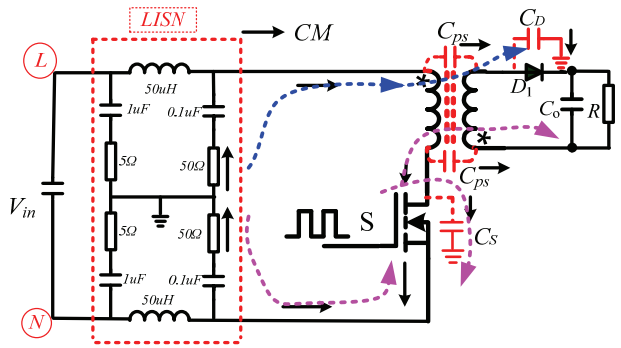

Fig. 1. Conducted CM EMI coupling path of a flyback converter.

conducted noise can be suppressed by using the transformer shielding technique in isolated converters [10]-[15]. In [11], [12], foil shielding and winding shielding techniques are utilized to cancel the CM current coupling path and to guarantee that the total CM current is minimized in the flyback converter, respectively. By proposing the concept of paired layers in the planar transformer structure, near-zero common mode noise is achieved in the flyback and forward converters in [15]. In addition, interleaved winding structures are adopted to reduce the ac resistance and leakage inductance of the PTs. Furthermore, the conduction losses and voltage spike of the power switch can be reduced. The winding cancellation method in [16], [17] is utilized in wire-wound transformers to cancel or alleviate common mode noise. However, such techniques increase the complexity of the topology or transformer structure. In addtion, the parameter design procedures for these methods are very difficult for electrical engineers.

Thirdly, noise source suppression techniques can be used to suppress the conducted CM EMI noise of isolated power converters [18]-[24]. In [18], the spread spectrum technique is utilized in a zero-current transition (ZCT) flyback converter to mitigate the CM EMI noise. In addition, an improved ZCT flyback converter is proposed in [19], and the conduction EMI was relieved by reducing of switching dv/dt and di/dt. Moreover, the passive lossless snubber [20], [21] was utilized in double-ended flyback converters to provide soft switching conditions for all of the semiconductor elements at turn on and turn off instants. By using the soft switching technique, the voltage stress of the power switch can be clamped and zero voltage turned on or zero current turned off are achieved. Thus, the efficiency of a converter can be improved. In [22], [23], the forward converter is modified to form a symmetric topology, and the conducted CM EMI noise can be reduced based on the balance concept. In [24], an analytical mathematical model of the common-mode (CM) EMI noise path is presented, and two improved layouts with self-supplied power control integrated circuits (ICs) are designed based on this model. However, the operational mode analysis of such converters is very complicated with an additional auxiliary switch or lossless snubber. In addition, and the cost of converter increased.

In a previous analysis, by applying the secondary technique to a soft switching half bridge DC-DC converter with an inductive output filter [25], a single-ended isolated converter using the secondary resonance technique is presented in this paper. By adding one diode and one resonant capacitor on the secondary-side of the traditional flyback converter, the voltage stress of the main power switch can be reduced and voltage across the output diode is clamped to the output voltage when compared to the conventional flyback converter. In addition, the peak current stress through the main power switch can also be decreased and zero current switching (ZCS) of the output diode can be achieved. Through the analysis, the conducted EMI noise source can be reduced while the common mode (CM) EMI noise and the differential mode (DM) EMI noise of such a converter are improved.

The remainder of this paper is organized as follows. In section II, the operational principle of the proposed converter is analyzed. The conducted EMI noise coupling path and its lumped-circuit EMI model along with the characteristics of the conducted EMI noise are described in section III. Simulation results of a 60W output power and a comparison analysis of the conducted EMI noise sources are given in section IV. An experimental prototype of the proposed converter is established and the results verify the theoretical analysis in section V. Finally, some conclusions are presented in section VI.

II. Operational Principle of the Single-Ended Isolated Secondary Resonant Converter

A. Circuit Configuration

The single-ended isolated resonant converter presented in [26], [27] is shown in Fig. 2. In this paper, a simplified analysis of the converter is derived and there is a focus on a detailed analysis of the EMI noise character performance. In order to simplify the analysis, some assumptions are made:

1) The power switches and diodes are ideal except for the anti-parallel diode and parasitic output capacitor.
2) The transformer is composed of a magnetizing inductor and a leakage inductor, with an ideal transformer with a turns ratio of n:1.
3) The output capacitor is so large that the voltage V_o can be considered as a constant in a switching period.

The isolated single-ended converter has four operational modes in one switching cycle and their corresponding equivalent circuits are shown in Fig. 3. Key waveforms of the proposed converter are shown in Fig. 4, where v_G is the gate pulse of the power switches, i_T and i_s are the currents through the primary-side and secondary-side of the transformer, respectively, v_{ds} is the voltage across the power switch S. In addition, v_{cr} is the voltage across the resonant capacitor C_r, while v_{D1}, v_{D2} and i_{D1}, i_{D2} are the voltage and current for the diodes D_1, D_2, respectively.

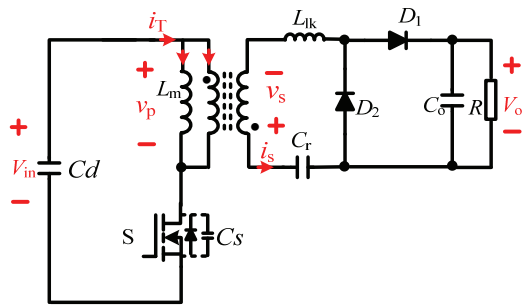

Fig. 2. Single-ended isolated secondary resonant converter.

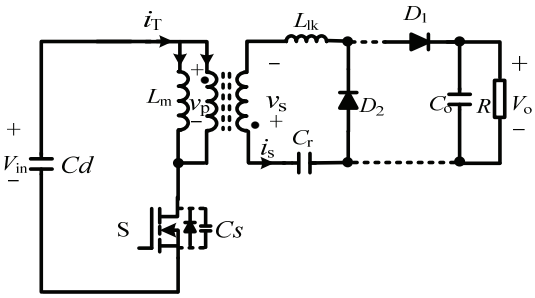

Mode 1 $[t_0 \sim t_1]$

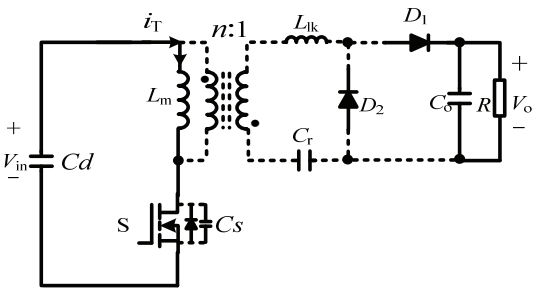

Mode 2 $[t_1 \sim t_2]$

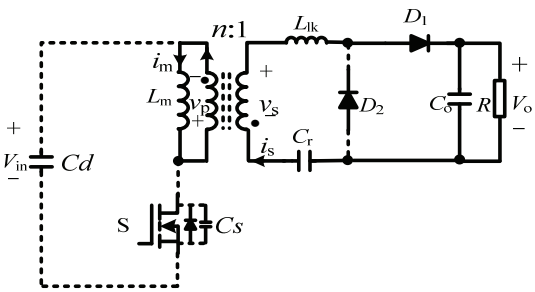

Mode 3 $[t_2 \sim t_3]$

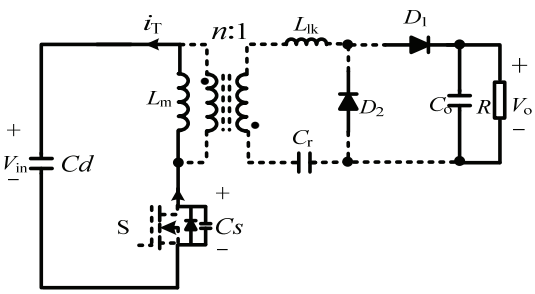

Mode 4 $[t_3 \sim t_4]$

Fig. 3. Equivalent circuits of the operational modes for the proposed converter.

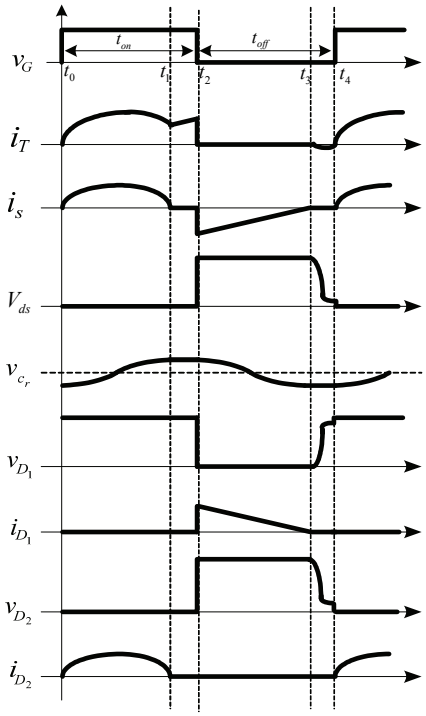

Fig. 4. Key waveforms of the proposed converter.

Mode 1 $[t_0 \sim t_1]$**:** At $t=t_0$, the gate pulse of the power switch S is arrived at and the switch S is turned on. Then the voltage across the magnetizing inductor of the transformer is equal to the input voltage V_{in}, and the current i_{Lm} increases linearly. Since it is operated in the discontinuous conduction mode (DCM) of the converter, the current through the magnetizing inductor Lm is zero at the beginning of one switching cycle. Thus, in this interval, the current i_{Lm} can be obtained as:

$$i_{L_m}(t) = \frac{V_{in}}{L_m}(t - t_0) \tag{1}$$

At the secondary side of the converter, the reflected voltage of the secondary-side of the transformer is negative and the diode D_2 conducts. The diode D_1 is turned-off due to the reverse-bias voltage across it. The capacitor C_r is charged by the current i_{Ls} and the diode D_2 provides the following path for the resonant circuit, which is composed of the inductor L_{lk}, the capacitor C_r, and the reflected voltage of the secondary–side of the transformer. In this mode, the circuit equation can be expressed as:

$$L_{lk}\frac{di_s(t)}{dt} = \frac{V_{in}}{n} - v_{C_r}(t) \tag{2}$$

$$i_s(t) = C_r\frac{dv_{C_r}(t)}{dt} \tag{3}$$

Based on equations (2) and (3), the following equation can be solved as:

$$i_s(t) = \frac{V_{in} - n \cdot v_{C_r}(t_0)}{n \cdot Z_{r1}} \sin \omega_{r1}(t - t_0) \tag{4}$$

$$v_{C_r}(t) = \frac{V_{in}}{n} + \left[v_{C_r}(t_0) - \frac{V_{in}}{n} \right] \cos \omega_{r1}(t - t_0) \tag{5}$$

Where, the character impedance Z_{r1} and angular frequency ω_{r1} can be defined as:

$$Z_{r1}=\sqrt{\frac{L_{lk}}{C_r}},\qquad \omega_{r1}=\frac{1}{\sqrt{L_{lk}C_r}} \tag{6}$$

After the half resonant period, the resonant current $i_s(t)$ returns to zero, the diode D_2 is turned off at zero current, and this mode ends. In this interval, the current i_p and the current i_T can be expressed as:

$$i_p(t)=\frac{1}{n}\cdot i_s(t)=\frac{V_{in}-n\cdot v_{C_r}(t_0)}{n^2\cdot Z_{r1}}\sin\omega_{r1}(t-t_0) \tag{7}$$

$$\begin{aligned} i_T(t)&=i_{L_m}(t)+i_p(t)\\ &=\frac{V_{in}}{L_m}(t-t_0)+\frac{V_{in}-n\cdot v_{C_r}(t_0)}{n^2\cdot Z_{r1}}\sin\omega_{r1}(t-t_0)\end{aligned} \tag{8}$$

Mode 2[t_1 ~t_2]: At $t=t_1$, the diode D_2 is turned off at zero current, the current i_{Ls} at the secondary-side of the transformer is kept zero, and the output capacitor C_o is discharge to the load. In addition, the power switch S is continuously conducted. Thus, the current i_{Lm} is increased linearly due to the clamped input voltage V_{in}. In this interval, the current through the switch can be expressed as:

$$i_T=i_{L_m}(t)=\frac{V_{in}}{L_m}(t-t_1)+i_{L_m}(t_1) \tag{9}$$

Mode 3[t_2 ~t_3]: At $t=t_2$, the power switch is turned off and the current i_T is suddenly returned to zero. At the secondary-side of the transformer, the diode D_1 is conducted to provide a following path for the magnetizing inductor current i_{Lm}. The output diode D_2 is turned off due to the reverse voltage. In this interval, the leakage inductor is in series with the magnetizing inductor. Thus, the leakage inductor is so small that can be neglected. The following circuit equation can be obtained as:

$$\frac{L_m}{n^2}\frac{di_s(t)}{dt}=V_o-v_{C_r}(t) \tag{10}$$

$$i_s(t)=C_r\frac{dv_{C_r}(t)}{dt} \tag{11}$$

Based on equations (10) and (11), the secondary side current $i_s(t)$ and the voltage across the capacitor C_r can be solved as:

$$i_s(t)=i_s(t_2)\cos\omega_{r2}(t-t_2)-Z_{r2}\left[v_{C_r}(t_2)-V_o\right]\sin\omega_{r2}(t-t_2) \tag{12}$$

$$v_{C_r}(t)=\left[v_{C_r}(t_2)-V_o\right]\cos\omega_{r2}(t-t_2)+\frac{i_s(t_2)}{Z_{r2}}\sin\omega_{r2}(t-t_2)+V_o \tag{13}$$

Where the character impedance Z_{r2} and the angular frequency ω_{r2} can be defined as:

$$Z_{r2}=n\sqrt{\frac{L_m}{C_r}},\qquad \omega_{r2}=\frac{1}{n\sqrt{L_mC_r}} \tag{14}$$

Since the resonant frequency is composed of the magnetizing inductor and the capacitor is much larger than the switching frequency, the voltage across the capacitor can be constant in this interval. Thus, the current $i_s(t)$ can be obtained as:

$$i_s(t)=n^2\frac{V_o-V_{C_r}}{L_m}(t-t_2)+i_s(t_2) \tag{15}$$

Mode 4[t_3 ~t_0]: At $t=t_3$, the current through the magnetizing inductor decreased to zero and the energy in the inductor L_m is completely released. Then the diode D_1 is turned off at zero current. In this mode, the secondary-side current $i_s(t)$ is kept zero and reflected to the primary-side of the transformer, and the current i_p is zero. Therefore, the transformer is disconnected from the primary-side and the output capacitor is discharged to the load. At the primary-side, the inductor L_m is clamped to the input voltage V_{in}. Solving the circuit equation and the current i_m can be expressed as:

$$i_m(t)=\frac{v_{C_s}(t_3)-V_{in}}{Z_{r3}}\sin\omega_{r3}(t-t_3) \tag{16}$$

$$v_{C_s}(t)=\left[v_{C_s}(t_3)-V_{in}\right]\cos\omega_{r3}(t-t_3)+V_{in} \tag{17}$$

$$Z_{r3}=\sqrt{\frac{L_m}{C_s}},\qquad \omega_{r3}=\frac{1}{\sqrt{L_mC_s}} \tag{18}$$

When the gate pulse of the power switch S is achieved and the next switching period begins.

III. Performance Analysis of the EMI Noise Characteristics of the Proposed Converter

A. Lumped-Circuit EMI Model of the Proposed Converter

a) Conducted CM EMI Analysis: The CM EMI noise coupling path of the proposed secondary resonance single-ended converter is shown in Fig. 5. The capacitors C_S and C_D are the equivalent parasitic capacitor to ground of the power switch and output diode, respectively. C_{ps} is the parasitic capacitor between the primary-side and secondary-side of the transformer. The Line Impedance Stabilization Network (LISN) is composed of the passive components in the dotted line box. Considering the parasitic capacitor of the power switch, the output diodes and the transformer, while the EMI noise sources can be considered as controlled voltage sources, the standard resistance of the LISN can be derived with a shorted-inductor and an opened-capacitor in the low frequency range. Therefore, a simplified CM EMI circuit model is shown in Fig. 6. Based on the circuit model in Fig. 6, a lumped-circuit model of the EMI noise source of the proposed converter can be obtained in Fig. 7. Z_{path} is equivalent impedance of the coupling path while L_{lk} and C_r are the resonant inductor and resonant capacitor, respectively.

It can be seen from Fig. 7 that there are three coupling paths for following through the LISN resistor, i.e. the parasitic capacitor of the power switch, the equivalent parasitic capacitor

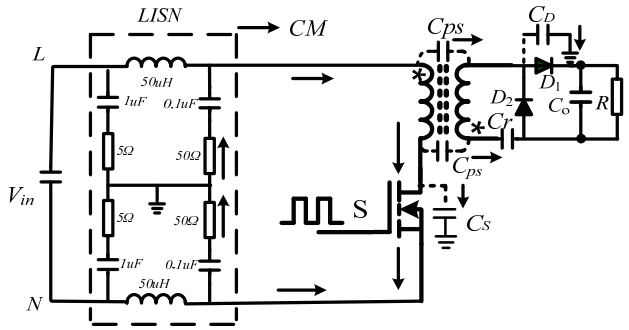

Fig. 5. Conducted CM EMI coupling path of the proposed converter.

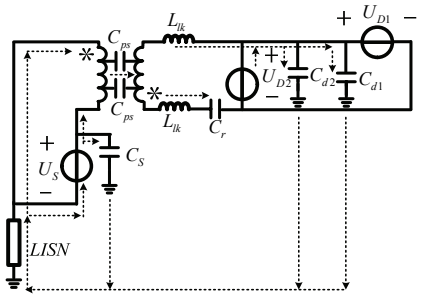

Fig. 6. Simplified CM EMI circuit model.

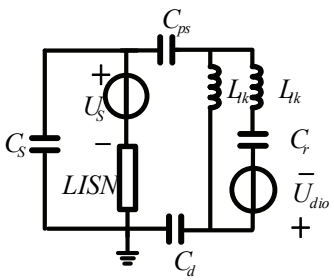

Fig. 7. Lumped-circuit model for CM EMI noise.

between in the primary and secondary of the transformer, and the output diode coupling path. In addition, it can be seen that C_s, C_{ps} and C_{d2} are the reason for the CM EMI noise. According to the superposition principle, the common mode voltage of the proposed converter can be expressed as:

$$U^*_{CM}(j\omega)=U^*_S(j\omega)\cdot\frac{R_{CM}}{\left[\left(j\omega L_{lk}+\frac{1}{j\omega C_r}\right)\|\, j\omega L_{lk}+\frac{1}{j\omega}\left(\frac{1}{C_{ps}}+\frac{1}{C_d}\right)\right]\|\frac{1}{j\omega C_s}+R_{CM}} \quad (19)$$

$$+U^*_{dio}(j\omega)\cdot\frac{j\omega L_{lk}}{j2\omega L_{lk}+\frac{1}{j\omega C_r}}\frac{\frac{1}{j\omega C_s}\|R_{CM}}{\frac{1}{j\omega}\left(\frac{1}{C_{ps}}+\frac{1}{C_d}\right)+\frac{1}{j\omega C_s}\|R_{CM}}$$

Where "||" represent parallel, i.e. x||y = (xy)/(x+y). In addition, R_{CM} is the CM equivalent impedance of the LISN.

b) Conducted DM EMI Analysis: The conducted DM EMI noise coupling path for the proposed converter is shown in Fig. 8. It can be seen that the DM EMI noise is propagated between line L and line N through the power switch, the primary-side of the transformer, and the LISN. The lumped-circuit model

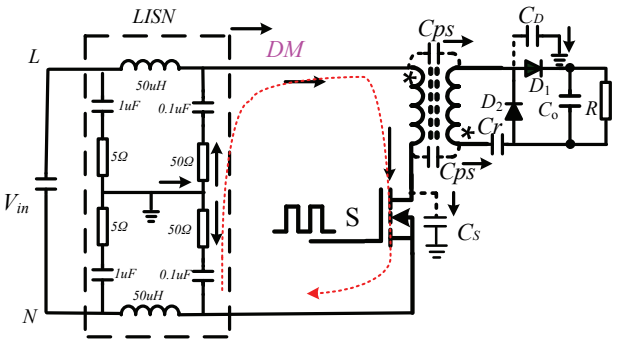

Fig. 8. Conducted DM EMI coupling path of the proposed converter.

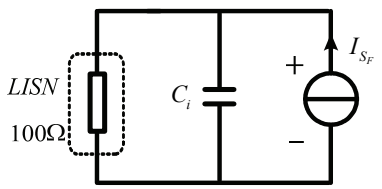

Fig. 9. Lumped-circuit model of the DM EMI noise.

for DM EMI noise can be simplified as shown in Fig. 9. Where, the DM EMI noise source can be considered as a controlled current source I_{sf}. This current source is shunted by the input capacitor C_{in} and the LSIN network. The differential mode voltage for the proposed converter can be expressed as:

$$U^*_{DM}(j\omega)=I^*_{S_R}(j\omega)\cdot\frac{\frac{1}{j\omega C_i}\cdot R_{DM}}{\frac{1}{j\omega C_i}+R_{DM}} \quad (20)$$

Where R_{DM} is the LISN equivalent resistor. It can be seen form equation (20) that the input capacitor can be shunted by the DM EMI noise source and that the DM voltage through the LISN resistor can be reduced through an appropriate selection of the capacitor value. In addition, the differential mode voltage is dominated by the current controlled source.

B. Reduced Equivalent CM EMI Noise Sources

It can be seen from the above analysis that the conducted CM noise is generated by semiconductor devices due to the fast switch action. The voltage across the main power switch in the proposed converter and the traditional flyback converter are shown in Fig. 10, which operated in the discontinuous conduction mode (DCM). In addition, $V_{s\_resonant}$ represents the voltage in the proposed converter, and $V_{s\_flyback}$ is the voltage in the flyback converter. Based on the analysis in section II, the peak voltage $V_{s\_resonant}$ of the power switch is equal to $V_{in}+(V_o-V_{Cr})/n$, where the average voltage across the resonant capacitor V_{Cr} can be considered to be a constant voltage with an adequate capacitor value. In addition, the peak voltage in the flyback converter is equal to $V_{in}+V_o/n$. Thus, from the point of view of the frequency domain analysis, the amplitude of the harmonics resonance for the power switch in the proposed

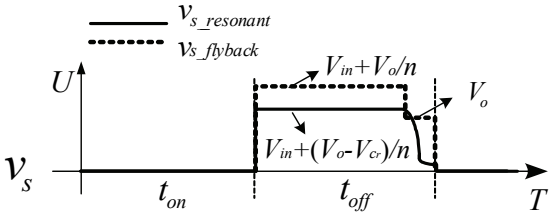

Fig. 10. Comparison analysis of the switch voltage in the traditional flyback converter and the proposed converter.

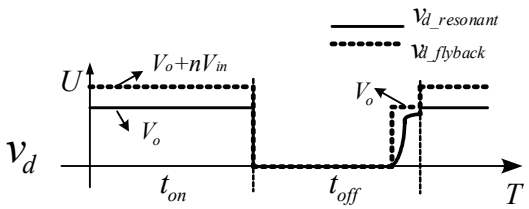

Fig. 11. Comparison analysis of the diode voltage in the traditional flyback converter and the proposed converter.

converter is smaller than that in the traditional flyback converter. In addition, the reduced CM EMI noise can be achieved in the proposed converter.

The diode voltage in the proposed converter and the traditional flyback converter are shown in Fig. 11. This figure shows that the diode voltage in the proposed converter is clamped to the output voltage, while the diode voltage across the traditional flyback converter is equal to V_o+nV_{in}. In addtion, it becomes even worse when considering the oscillation between the parasitic capacitor with the leakage inductor of the transformer. Therefore, the CM EMI noise generated by the output diode can be reduced in the proposed converter when compare with the flyback converter.

Based on the above analysis, the conducted CM EMI noise sources composed of the power switch voltage source and the diode voltage source in the proposed converter can be reduced. Thus, the CM EMI noise can also be reduced.

C. Reduced Equivalent DM EMI Noise Sources

It can be seen from Fig. 9 that the conducted DM EMI noise is generated by the switch current EMI noise source between line *L* and line *N*. Using the secondary resonance technique, the peak current through the primary-side power switch can be expressed as:

$$i_{L\_A}=\frac{V_{in}}{L_m}\cdot t_{on} \tag{21}$$

$$i_{L\_B}=\frac{V_{in}}{L^*_m}\cdot t_{on} \tag{22}$$

where, the values L_m and L_m^* are the magnetizing inductors of the transformer in the traditional flyback converter and proposed converter as shown in Fig. 12.

When operating at the same input voltage and switch frequency, the difference in the switch current is determined

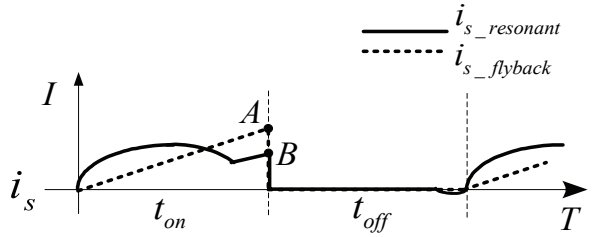

Fig. 12. Switch current waveforms in the traditional flyback converter and the proposed converter.

by the magnetizing inductor value of the transformer. In the traditional Flyback converter, the energy is stored in the on-time interval and released to the load in the off-time interval. Therefore, the transferred energy can be obtained as $W_F=1/2*L_m*i^2_{L\_A}$. However, in the proposed converter, the inductor L_m^* is charged and the energy is stored in the capacitor C_r in the on-time interval, and release to the load through the energy by a series connection of the inductor $L_m^*$and capacitor Cr. As a result, $W_R=1/2*L^*_m*i^2_{L\_B}+\Delta W_{Cr}$.

Considering a transfer of the same output power, $W_R=W_F$, it can be obtained as:

$$\frac{1}{2}L_m\cdot i^2_{L\_A}=\frac{1}{2}L^*_m\cdot i^2_{L\_B}+\Delta W_{C_r} \tag{23}$$

Due to $\Delta W_{Cr}>0$:

$$\frac{1}{2}L_m\cdot i^2_{L\_A}>\frac{1}{2}L^*_m\cdot i^2_{L\_B} \tag{24}$$

Based on the equations (21), (22) and (24), it can be obtained as:

$$\frac{1}{2}\frac{V^2_{in}}{L_m}\cdot t^2_{on}>\frac{1}{2}\frac{V^2_{in}}{L^*_m}\cdot t^2_{on} \tag{25}$$

Thus, $L_m<L^*_m$, $i_{L\_A}>i_{L\_B}$. Therefore, during the off-time interval, the di/dt of the current source is reduced when compared to the traditional flyback converter, i.e. $U^*_{DM}(j\omega)<U_{DM}(j\omega)$, and the DM EMI noise can be reduced.

IV. Simulation Results

According to the above analysis, a simulation prototype with 60W/60V is established in Saber software. For comparison, the same specification parameters of the traditional flyback converter are given.

A comparison of the CM EMI noise in the traditional flyback converter and the proposed converter with the secondary resonance technique are shown in the Fig. 13, where "fly" represents the traditional flyback converter and "res" represents the proposed converter with the secondary resonance technique. In Fig. 13(a) with an output power of P_o=20W, the CM EMI noise of the proposed converter is reduced by about 2dBuV when compared to the conventional flyback converter, and this technique has little effect on the

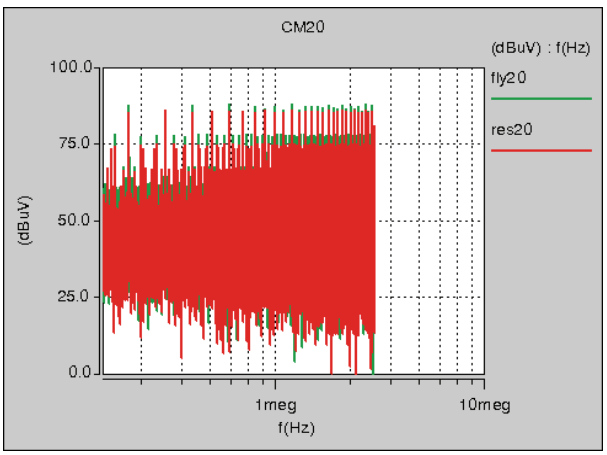

(a)

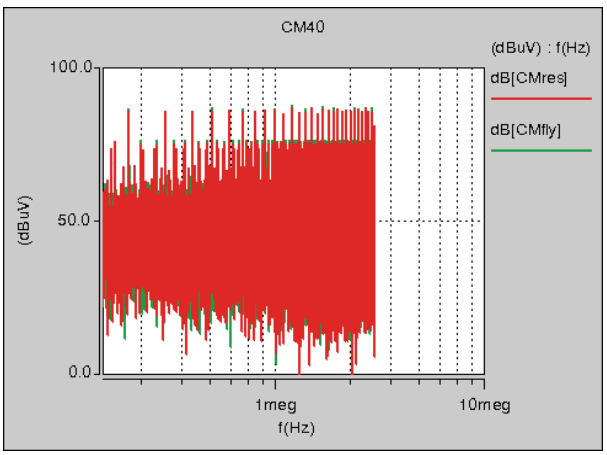

(b)

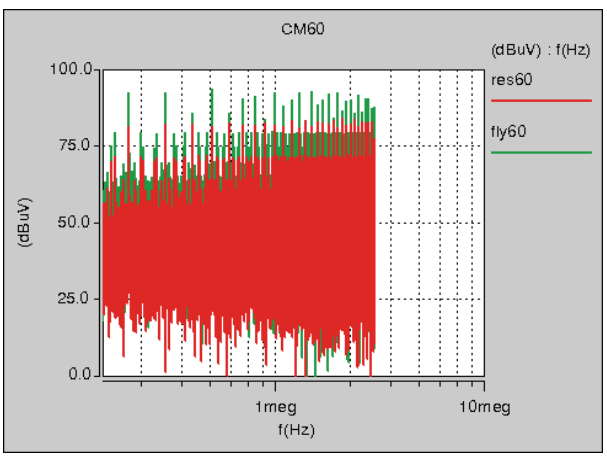

(c)

Fig. 13. Comparison analysis of CM EMI noise in the flyback converter and the proposed converter at different output powers. (a) P_o=20W. (b) P_o=40W. (c) P_o=60W.

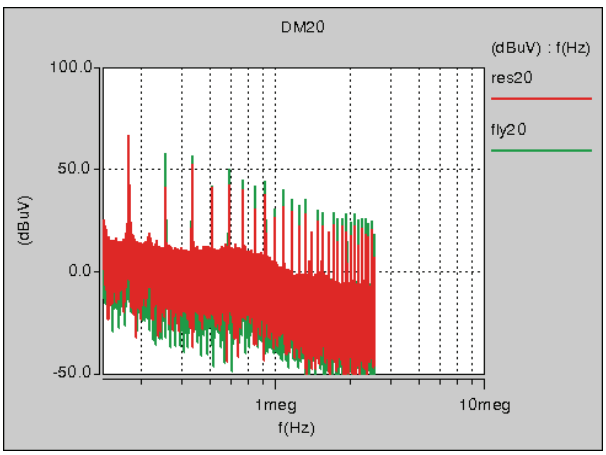

(a)

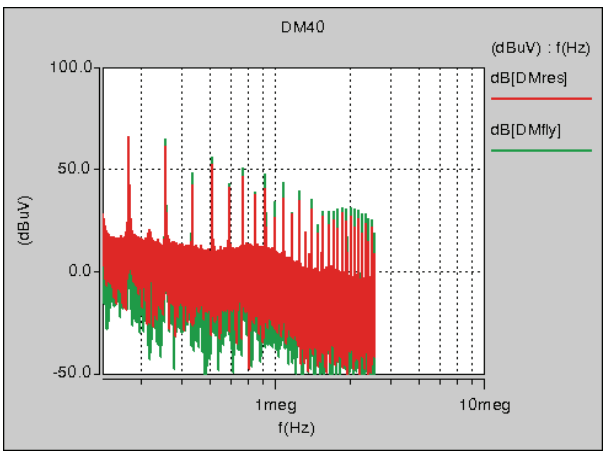

(b)

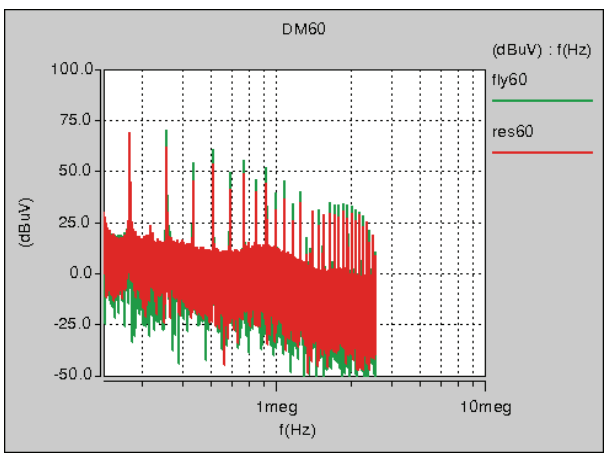

(c)

Fig. 14. Comparison analysis of DM EMI noise in the flyback converter and the proposed converter at different output powers. (a) P_o=20W. (b) P_o=40W. (c) P_o=60W.

CM EMI noise. The same phenomena appear in Fig. 13 in the frequency range of 150kHz~3.0MHz. However, it can be seen from Fig. 13(c) that the CM EMI noise of the proposed converter with the secondary resonance technique are reduced by 10 dBuV, 12 dBuV and 12dBuV at 300kHz, 500kHz and 1.5MHz, respectively. The simulation results indicate that the proposed converter with the secondary resonance technique can improve the CM EMI noise in the low frequency range.

Fig. 14 shows the DM EMI noise of the conventional flyback converter and the proposed converter with the secondary resonance technique. It can be seen from Fig. 14 that the DM EMI noise of the proposed converter is reduced by about

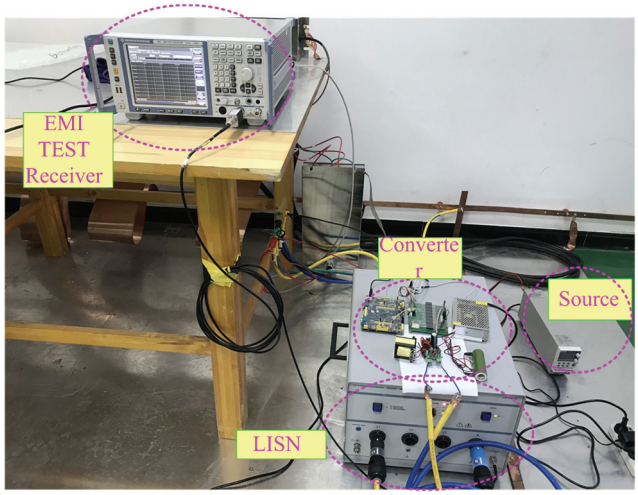

Fig. 15. EMI test platform of the proposed resonant single-ended converter.

8dBuV at the low frequency range. In addition, the DM EMI noise can be reduced in the wide frequency range of 150 kHz~3.0MHz. Thus, by introducing the secondary resonance technique, the characteristic of the DM EMI noise can be improved.

V. Experimental Results

A. Design Example

In order to verify the theoretical analysis, an experimental prototype of the proposed converter with the secondary resonance technique and the traditional flyback converter are established. The specification parameters of these converters are: input voltage V_{in}=17V, output voltage V_o=60V, output power P_o=60W, resonant capacitor C_r=0.45μF, output filter capacitor C_o=330μF, and switching frequency f_s=50kHz. The turns-ratio of the transformer is selected as n_1:n_2=1/3, the duty cycle for the main power switch is D=0.4, and the secondary leakage inductor of the transformer is L_k=2.7μH. The main power switch is selected as P75NF75, and the output diodes D_1 and D_2 are selected as MUR10100.

An EMI test platform of the proposed resonant single-ended converter is built in the laboratory and shown in Fig. 15.

B. EMI Test Results

According to the above parameters of the proposed converter, EMI test results of the traditional flyback converter and the single-ended resonant converter are shown in Fig. 16 and Fig. 17, respectively. It can be seen in Fig. 16 – Fig. 17 that the proposed resonant converter has advantages over the traditional flyback converter in the medium frequency range, especially the 1~3MHz frequency range. However, in the low frequency range, the proposed resonant technique has little effect on the EMI of the single-ended isolated converter. This is due to the fact that in the proposed converter, the frequency spectra of the equivalent controlled voltage sources and the

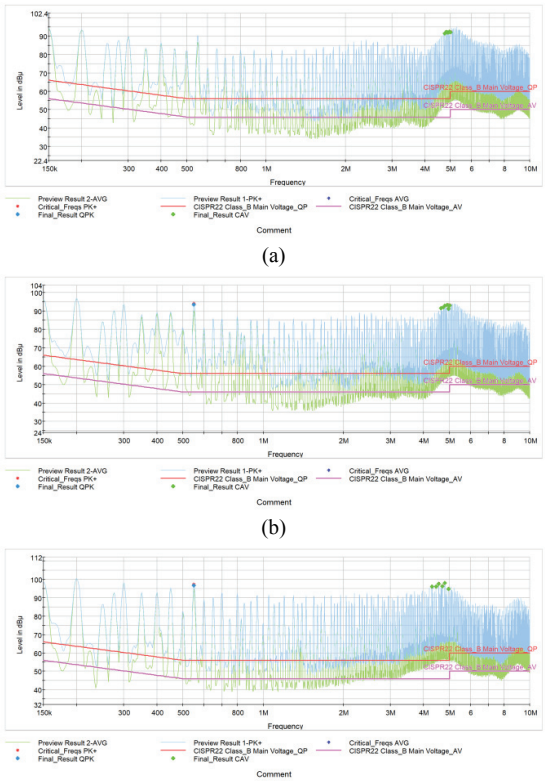

Fig. 16. EMI test results of the traditional flyback converter. (a) P_o=20W. (b) P_o=40W. (c) P_o=60W.

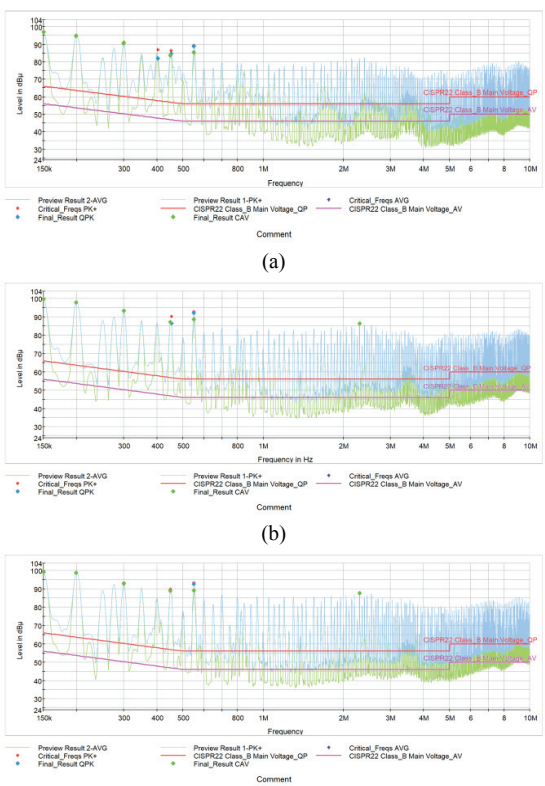

Fig. 17. EMI test results of the proposed single-ended isolated resonant converter. (a) P_o=20W. (b) P_o=40W. (c) P_o=60W.

controlled current source are decreased when compared with the traditional flyback converter in the medium frequency range. In addition, appropriate parameter selection of the resonant circuit network can increase the equivalent impedance in the EMI coupling path in the low frequency range. Thus, the EMI of the proposed converter has been improved.

VI. CONCLUSIONS

This paper studies the single-ended isolated converter using the secondary resonance technique and its operational principle along with the EMI noise source and its coupling path. In addition, the lumped-circuit model of the EMI noise is described. Based on the equivalent model, the common-mode voltage and differential-mode voltage of the proposed converter are analyzed. The analysis results show that by using the secondary resonance technique, common mode noise sources are reduced and that the CM EMI noise can be improved by selecting an appropriate impedance of the resonant circuit network. In addition, the DM EMI noise is reduced with a decrement of the current spectra. From simulation and experiment results, it can be seen that the maximum common-mode noise is reduced by 12dBuV, and the differential mode noise is reduced by 8dBuV. Based on these merits, the proposed converter with the secondary-side resonant technique can be utilized in small and medium power applications with a low EMI level.

ACKNOWLEDGMENT

This work was supported by the National Natural Science Foundation of China under grant no.51607027, the Fundamental Research Funds for the Central Universities under project number ZYGX2016KYQD123, and the Scientific and Technical Supporting Programs of Sichuan Province under Grant (2016GZ0395, 2017GZ0395 and 2017GZ 0394).

REFERENCES

[1] L. Yiming, W. Shuo, H. Sheng, C. ChoonPing, and L. Srikanth. "Investigating CM voltage and its measurement for AC/DC power adapters to meet touchscreen immunity requirement," *IEEE Trans. Electromagn. Compat.,* Vol. 60, No. 4, pp. 1102-1110, Aug. 2018.

[2] C. Korte, E. Specht, and S. Goetz, "A novel spectral control method for an automotive gallium nitride DC-DC converter," *Intelligent Motion, Renewable Energy and Energy Management (PCIM)*, pp. 1-7, 2017.

[3] J. J. Shieh, Y. H. Chao, and W. Chuang. "A family of off-line SMPSs used in FCL with reducing secondary-side CM noise," *Annual Conference of the IEEE Industrial Electronics Society (IECON)*, pp. 193-197, 2013.

[4] G. Spiazzi, P. Mattavelli, and A. Costabeber, "High step-up ratio flyback converter with active clamp and voltage multiplier," *IEEE Trans. Power Electron.,* Vol. 26, No. 11, pp. 3205-3214, Nov. 2011.

[5] W.Cheng, Z. Huang, S. Xu, and W. Sun, "Novel Hybrid Analytical/Numerical Conducted EMI Model of a Flyback Converter", *IEEE Trans. Electromagn. Compat.*, Vol. 59, No. 2, pp. 488-497, Apr. 2017.

[6] P. Meng, J. Zhang, H. Chen, Z. Qian, and Y. Shen, "Characterizing noise source and coupling path in flyback converter for common-mode noise prediction," *Applied Power Electronics Conference and Exposition (APEC)*, pp. 1704-1709, 2011.

[7] M. R. Yazdani, H. Farzanehfard, and J. Faiz, "Classification and comparison of EMI mitigation techniques in switching power converters - A review," *J. Power Electron.,* Vol. 11, No. 5, pp. 767-777, Sep. 2011.

[8] K. Mainali and R. Oruganti, "Conducted EMI mitigation techniques for switch-mode power converters: A survey," *IEEE Trans. Power Electron.,* Vol. 25, No. 9, pp. 2344-2356, Sep. 2010.

[9] D. Hamza, M. Sawan, and P. K. Jain, "Suppression of common-mode input electromagnetic interference noise in DC–DC converters using the active filtering method," *IET Power Electron.,* Vol. 4, No. 7, pp. 776-784, Aug. 2011.

[10] P. Kong and F. C. Lee, "Transformer structure and its effects on common mode EMI noise in isolated power converters," *Applied Power Electronics Conference and Exposition (APEC)*, pp. 1424-1429, 2010.

[11] H. Chen and J. Xiao, "Determination of transformer shielding foil structure for suppressing common-mode noise in flyback converters," *IEEE Trans. Magn.*, Vol. 52, No. 12, pp. 1-9. Dec. 2016.

[12] Y. P. Chan, B. M. H. Pong, N. K. Poon, and J. C. P. Liu, "Common-mode noise cancellation by an antiphase winding in multilayer isolated planar transformer," *IEEE Trans. Electromagn. Compat.*, Vol. 56, No. 1, pp. 67-73, Feb. 2014.

[13] S. Yang, Q. Chen, and W. Chen, "Common mode EMI noise reduction technique by shielding optimization in isolated converters," *Asia-Pacific International Symposium on Electromagnetic Compatibility (APEMC),* pp. 622-625, 201.

[14] B. G. Kang, S. K. Chung, J. S. Won, and H. S. Kim, "EMI reduction technique of flyback converter based on capacitance model of transformer with wire shield," *International Conference on Power Electronics and ECCE Asia (ICPE-ECCE Asia)*, pp. 163-169, 2015.

[15] M. A. Saket, M. Ordonez, and N. Shafiei, "Planar Transformers with near-zero common-mode noise for flyback and forward converters," *IEEE Trans. Power Electron.*, Vol. 33, No. 2, pp. 1554-1571, Feb. 2018.

[16] J. Stahl, S. Wieczorek, M. Schmidt, M. Albach, "Effective CM reduction in a flyback by means of passive cancellation," *IEEE ECCE Asia Downunder (ECCE Asia)*, pp. 1137-1143, 2013.

[17] D. Cochrane, D. Y. Chen, and D. Boroyevic, "Passive cancellation of common-mode noise in power electronic circuits," *IEEE Trans. Power Electron.*, Vol. 18, No. 3, pp. 756-763, May 2003.

[18] M. R. Yazdani and H. Farzanehfard, "Conducted electromagnetic interference analysis and mitigation using zero-current transition soft switching and spread spectrum techniques," *IET Power Electron.,* Vol. 5, No. 7, pp. 1034-

1041, Aug. 2012.
[19] M. R. Yazdani, H. Farzanehfard, and J. Faiz, "EMI analysis and evaluation of an improved ZCT flyback converter". *IEEE Trans. Power Electron.*, Vol. 26, No. 8, pp. 2326-2334, Aug. 2011.
[20] M. R. Yazdani, S. Rahmani, and M. Mohammadi, "A ZCT double-ended flyback converter with low EMI," *J. Power Electron.*, Vol. 15, No. 3, pp. 602-609, May 2015.
[21] M. Mohammadi, E. Adib, and H. Farzanehfard, "Passive lossless snubber for double-ended flyback converter," *IET Power Electron.* Vol. 8, No. 1, pp. 56-62, Jan. 2014.
[22] M. R. Yazdani, N. A. Filabadi, and J. Faiz, "Conducted electromagnetic interference evaluation of forward converter with symmetric topology and passive filter," *IET Power Electron.,* Vol. 7, No. 5, pp. 1113-1120, May 2013.
[23] P. Kong, S. Wang, F. C. Lee, and Z. Wang, "Reducing common-mode noise in two-switch forward converter," *IEEE Trans. Power Electron*., Vol. 26, No. 5, pp. 1522-1533, May 2011.
[24] W. Cheng, X. He, S. Xu, and W. Sun, "Analysis of common-mode electromagnetic interference noise in a flyback converter using a self-supply power control integrated circuit," *IET Power Electron*., Vol. 8, No. 9, pp. 1749-1757, Sep. 2015.
[25] Z. Y. Chen and Y. Chen, "A secondary resonance soft switching half bridge DC-DC converter with an inductive output filter," *J. Power Electron*., Vol. 17, No. 6, pp. 1391-1401, Nov. 2017.
[26] J. M. Kwon, W. Y. Choi, and B. H. Kwon, "Single-switch quasi-resonant converter," *IEEE Trans. Ind. Electron*., Vol. 56, No. 4, pp. 1158-1163, Apr. 2009.
[27] K. B. Park, C. E. Kim, G. W. Moon, and M. J. Youn, "PWM resonant single-switch isolated converter," *IEEE Trans. Power Electron*., Vol. 24, No. 8, pp. 1876-1886, Aug. 2009.

Zhangyong Chen was born in Sichuan, China, in 1988. He received his B.S. degree in Electrical Engineering and its Automation, and his Ph.D. degree in Electrical Engineering from Southwest Jiaotong University (SWJTU), Chengdu, China, in 2010 and 2015, respectively. From September 2014 to September 2015, he was a Visiting Student in the Future Energy Electronics Center (FEEC), Virginia Tech, Blacksburg, VA, USA. Since January 2016, he was been a Lecturer in the School of Energy Science and Engineering, and since July 2018, he has been an Associate Professor in the School of Automation Engineering, University of Electronic Science and Technology of China (UESTC), Chengdu, China. His current research interests include switching-mode power supplies, soft switching techniques, power factor correction converters and renewable energy sources.

Yong Chen (SM'16, M'08) was born in Sichuan, China, in 1977. Since 2015, he has been a Professor and a Ph.D. Supervisor in the School of Energy Science and Engineering, and a Professor in the School of Automation Engineering, University of Electronic Science and Technology of China (UESTC), Chengdu, China. He also served as the Director of the Institute for Electric Vehicle Driving Systems and Safety Technology, UESTC. He was a Visiting Scholar in School of Mechanical Engineering, University of Adelaide, Adelaide, SA, Australia. Since Jan. 2018, he has been presiding over a National Natural Science Foundation of China project and over Scientific and Technical Supporting programs in Sichuan Province. He has published over 50 technical papers in journals and conference proceedings. In addition, he has 15 Chinese patents. His current research interests include power electronics, motor control, energy control and network control. He is a Senior Member of the IEEE, and a Member of the Chinese Society for Electrical Engineering (CSEE).

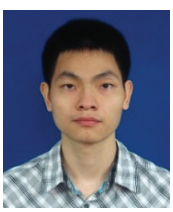

Qiang Chen was born in Guangxi, China, in 1992. He received his B.S. degree in New Energy Materials and Devices, and his M.S. degree in Control Engineering from the School of Automation Engineering, University of Electronic Science and Technology of China (UESTC), Chengdu, China, in 2015 and 2018, respectively. His current research interests include switching-mode power supplies and soft switching techniques.

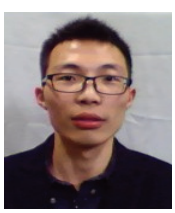

Wei Jiang was born in Sichuan, China, in 1993. He received his B.S. degree in Electrical Engineering from the School of Electrical Engineering and Electronic Information, Xihua University, Chengdu, China, in 2017. He is presently working towards his M.S. degree in Control Engineering from the School of Automation Engineering, University of Electronic Science and Technology of China (UESTC), Chengdu, China. His current research interests include switching-mode power supplies and soft switching techniques.

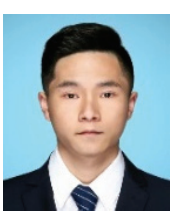

Rongqiang Zhong was born in Sichuan, China, in 1995. He received his B.S. degree in Smart Grid and Information Engineering from the School of Mechanical and Electrical Engineering, University of Electronic Science and Technology of China (UESTC), Chengdu, China, in 2014, where he is presently working towards his M.S. degree in Electrical Engineering. His current research interests include DC-DC converter and digital control techniques.